Lattice models of advection-diffusion

Raymond T. Pierrehumbert
University of Chicago, Chicago, Illinois

(Received 10 May 1999; accepted for publication 10 November 1999)

We present a synthesis of theoretical results concerning the probability distribution of the concentration of a passive tracer subject to both diffusion and to advection by a spatially smooth time-dependent flow. The freely decaying case is contrasted with the equilibrium case. A computationally efficient model of advection-diffusion on a lattice is introduced, and used to test and probe the limits of the theoretical ideas. It is shown that the probability distribution for the freely decaying case has fat tails, which have slower than exponential decay. The additively forced case has a Gaussian core and exponential tails, in full conformance with prior theoretical expectations. An analysis of the magnitude and implications of temporal fluctuations of the conditional diffusion and dissipation is presented, showing the importance of these fluctuations in governing the shape of the tails. Some results concerning the probability distribution of dissipation, and concerning the spatial scaling properties of concentration fluctuation, are also presented. Though the lattice model is applied only to smooth flow in the present work, it is readily applicable to problems involving rough flow, and to chemically reacting tracers. © *2000 American Institute of Physics.* [S1054-1500(00)02201-1]

The evolution of the concentration field of a nonreacting chemical substance (a ''passive tracer'') subject to rearrangement by advection and by molecular diffusion presents a rich variety of questions of deep theoretical interest. Advection-diffusion is also central to a variety of problems of considerable practical importance, such as combustion, and atmospheric chemistry. The probability distribution, or histogram of the tracer concentration field, provides much information about the mixing process, and has been the subject of much numerical and theoretical attention. We survey progress that has been made in understanding the PDF for the case of advection-diffusion by smooth flow, expose some remaining gaps in the current understanding, and point out a few aspects of the problem that have not hitherto been sufficiently appreciated. In addition, a computationally efficient lattice-based model problem suitable for exploratory inquiries into the subject is introduced. The utility of the method is illustrated through applications to spatially smooth advection of a nonreactive tracer, and suggestions are made for extensions to problems where the theoretical underpinnings are not so well developed.

I. INTRODUCTION

The advection-diffusion problem has been the subject of intense interest because it makes an appearance in a wide range of physical phenomena about which one would like to make predictions. Equally, the advection diffusion problem serves as a testbed for ideas on the statistical structure of turbulence, since it offers many of the same mathematical challenges, but in a setting that is not quite so demanding as the fully nonlinear Navier–Stokes equations. We shall be concerned with the statistical properties of a scalar tracer advected by a specified time-dependent flow field, and subject to sources and to mixing by diffusion. Such a tracer is governed by the nondimensional equation

$$\frac{\partial \theta}{\partial t} + \mathbf{v} \cdot \nabla \theta = \mathrm{Pe}^{-1} \nabla^2 \theta + f, \tag{1}$$

where θ is the concentration, $\mathbf{v}$ is the velocity, Pe is the Peclet number, and f is a source of tracer variance. The Peclet number is a measure of the strength of the diffusivity and is defined as UL/κ, where U is the typical velocity scale of the advecting flow, L is its typical length scale, and κ is the diffusivity of the tracer. We will confine attention to the case where $\mathbf{v}$ is nondivergent, and will be most interested in the weakly diffused case, i.e., large Pe. Because of the scale-selective dissipation, the diffusion acts strongly on sufficiently small scales even though Pe is large. The equation (1) gets interesting precisely because the straining action of the velocity continually creates fluctuations in θ of a spatial scale small enough to be dissipated. It will be assumed that the average of f over the entire domain vanishes, so that in a well-mixed state there is no tendency for the mean value of θ to grow without bound. Attention will be confined to the two-dimensional case, though many of the techniques and arguments admit ready generalizations to three dimensions. Throughout, we employ Cartesian coordinates (x,y) with corresponding velocity components (u,v).

In the limit of infinite Pe and vanishing f, Eq. (1) states simply that the value of θ is conserved following trajectories. A large literature on the properties of chaotic trajectories induced by incompressible time-dependent flow in 2D has built up, and the subject generally goes by the name ''chaotic advection.'' Tracer rearrangement by pure advection causes the probability distribution function (hereafter ''PDF'') of the gradient of θ to evolve, but it leaves the PDF of θ, $P(\theta)$, invariant. Introducing diffusivity to the problem makes it

considerably richer, since fluid parcels can exchange tracer with their neighbors, leading to evolution of the PDF of θ. This PDF is the object of first interest in many applications, and it will be our prime concern in the following. Much of what has been learned about the generation of tracer gradients from the study of pure chaotic advection will prove of great utility in the study of how $P(\theta)$ evolves. A very complete understanding of the tracer evolution is available for the case of advection by random unidirectional shear, and also for general flows in the limit where the spatial scale of the tracer variation is much larger than that of the advecting flow (the ''homogenization problem'').[1] In the present work, we concentrate on the case in which the underlying advection problem yields chaotic trajectories, and we do not impose any particular restriction on the spatial scale of the tracer fluctuation.

Numerical experimentation is an important means of formulating and testing conjectures in the less explored areas regarding the statistics of (1). The case of random advection by smooth flow is the best understood from a theoretical standpoint, but even there, major gaps remain in the understanding of the shape and evolution of $P(\theta)$. One purpose of this paper is to introduce a computationally efficient model problem for the study of advection-diffusion, and to illustrate its utility in probing the major theoretical questions in the context of random advection by smooth flow. First, we survey the basic theoretical underpinnings concerning $P(\theta)$ in Sec. II, taking time to tie up some loose ends regarding the smooth flow case. The numerical model is described in Sec. III. Numerical results for smooth flow are given in Sec. IV; for the most part, these concern $P(\theta)$, but we also provide a few results concerning the PDF of the tracer gradient, and concerning the lack of anomalous scaling of the tracer field. Though the numerical algorithm is applied here only to the smooth flow case, it can also be used to probe the behavior of systems for which the state of understanding is much more rudimentary, notably the case of advection by flows with singular velocity gradients, and problems involving chemical reactions. A few such suggested extensions are outlined in Sec. V.

II. THEORETICAL PRELIMINARIES CONCERNING THE PDF

A. General considerations

In the limit of vanishing dissipation and forcing, (1) reduces to the statement that the value of θ is conserved following fluid trajectories. Therefore, it is no surprise that the associated Lagrangian trajectory problem

$$\frac{dx}{dt}=u(x,y,t), \quad \frac{dy}{dt}=v(x,y,t) \tag{2}$$

should play an important role in the limit of weak diffusivity, i.e., large Pe. The behavior of (2) enters into the statistics of the solution of (1) primarily through the statistics of the *finite time Lyapunov exponents* (abbreviated FTLEs). For two-dimensional flows, the meaning of the FTLEs can be grasped by placing an infinitesimal disk of dye, with radius ϵ at a point (x_0,y_0) at time t_0, and allowing it to be advected by the flow for a length of time T. If ϵ is sufficiently small and the velocity gradients are always finite, then the disk will be distorted into an ellipse with semi-major and minor axes L_1 and L_2. If the flow is nondivergent, $L_1L_2=\epsilon^2$, and the straining is characterized by the expansion rate alone. From this, we define the FTLE for the given time interval and the given initial point as the small ϵ limit of

$$\Lambda(x_0,y_0,t_0,T)=T^{-1}\ln(L_1/\epsilon). \tag{3}$$

The FTLEs for incompressible flow, defined in this fashion, are either positive or zero. Note that vanishing Λ in the limit of small ϵ still allows for algebraic growth of the major axis of the ellipse, as occurs in steady shear flow and other regions of invariant tori. The FTLEs are well defined for all trajectories if the flow field is spatially smooth, by which we mean that the velocity gradients are everywhere finite. If the kinetic energy spectrum of the advecting flow field is shallower than k^{-3} at large wave number k, then the velocity gradients are generally singular at some points. A fundamentally different approach, perhaps based on the rate of separation of trajectories initially a small but *finite* distance apart, may be needed for the characterization of mixing in such flows. The definition of Λ in (3) continues to exist for any finite ϵ, but it diverges for small ϵ for trajectories that spend a sufficiently long time near a singularity of the gradient.

The quantity of interest is the probability distribution of Λ over an ensemble of trajectories obtained by integrating (2) for a fixed length of time T beginning from a suitable collection of initial conditions (x_o,y_o,t_o). One common choice for the ensemble is to sample the space of all initial conditions with a regular or random collection of (x_o,y_o), and carry out all integrations starting at $t_o=0$. Another choice is to take a single very long trajectory starting at a particular (x_o,y_o), and to make the ensemble out of segments of the trajectory of length T. If the system is nonergodic, or if the ergodic relaxation time is longer than T, the choice of ensemble affects the outcome. We shall refer to the PDF of the FTLEs as $Q(\Lambda,T)$. For two-dimensional spatially smooth flow whose associated trajectory problem (2) is ergodic in the whole spatial domain, it has been shown[2] that for large T

$$Q(\Lambda,T)=\sqrt{\frac{aT}{\pi}}e^{-aT(\Lambda-\bar{\Lambda})^2}, \tag{4}$$

provided that Λ is not extremely far from its most probable value $\bar{\Lambda}$. In (4), the coefficient a is a constant characterizing the overall level of velocity gradient fluctuations in the advecting flow. The method used by Chertkov *et al.*[2] for proving this is very specific to two dimensions. Nonergodic behavior, arising from invariant tori, cantorii and other transport barriers, leads to significant deviations from Gaussianity. In particular, the phenomenon of ''sticking'' to invariant tori at the boundary of a chaotic region is known to lead to anomalously large probabilities of low Λ.[3] Although analytic results like (4) may not be generally available, the fact remains that an evaluation of $Q(\Lambda,T)$, by numerical means if necessary, is the starting point for the analysis of the mixing properties of any novel smooth flow one may wish to treat.

When Λ is nonzero, and hence positive, any gradients initially present in the tracer distribution are amplified exponentially. The point of contact with the diffusive problem is made by examining the scale at which the amplification of gradients by strain is balanced by diffusion. In nondimensional terms, this scale is

$$l_* = (\Lambda \mathrm{Pe})^{-1/2}. \tag{5}$$

An initially large scale structure will cascade down to this dissipation scale, and thereafter not get any smaller. Because there is a range of values of Λ characterized by $Q(\Lambda, T)$, there is a range of dissipation scales over the domain. It takes a finite time for tracer fluctuations to cascade down to the dissipation scale. If the initial scale is L, then the time for dissipation to set in is

$$t_* = \Lambda^{-1} \ln(L/l_*) \tag{6}$$

on account of the exponential amplification of the gradients. Because of the fluctuations in Λ, there is a range of t_*; the fluctuations of the dissipation time are governed primarily by the prefactor Λ^{-1}, rather than by the fluctuations in l_*, which affects the dissipation time only logarithmically. Information on the fluctuations of l_* and t_* can be used systematically to obtain information on the statistics of the tracer field, as was done for the white-noise forced case by Chertkov *et al.*[2] Shortly, we will pursue the same enterprise more simply, though less rigorously.

Another approach to determining $P(\theta)$ is to derive the transport equation governing the PDF. The use of PDF transport equations has a long and well-developed history in the combustion and chemical engineering literature,[4,5] and many of the ideas that became popular during the recent revival of interest in PDF approaches to advection-diffusion in fact had their first expression in that literature. Sinai and Yakhot[6] indirectly adopted the PDF transport approach, by forming a heirarchy of equations governing the moments $\langle \theta^q \rangle$. It has been shown[7] that the transport equation can be easily derived by noting that $P(Z,t) = \langle \delta(Z - \theta(x,y,t)) \rangle$, where angle brackets denote a spatial average and Z is a dummy variable. The transport equation follows by taking the time derivative of this expression for $P(Z,t)$ and systematically making use of the fact that θ satisfies (1). The result is

$$\partial_t P = -\mathrm{Pe}^{-1} \partial_\theta \{ P(\theta) \langle \nabla^2 \theta \rangle_\theta \} - \partial_\theta \{ P(\theta) \langle f \rangle_\theta \} \tag{7}$$

$$= -\mathrm{Pe}^{-1} \partial_{\theta\theta} \{ P(\theta) \langle |\nabla \theta|^2 \rangle_\theta \} - \partial_\theta \{ P(\theta) \langle f \rangle_\theta \}, \tag{8}$$

where $\langle \cdots \rangle_\theta$ represents the conditional average of the indicated quantity over all parts of the domain where θ takes on the specified value. The advection terms affect the PDF only through their effect on the conditioned diffusion and forcing. The hard part of the problem is coming up with a theory of the conditioned diffusion or dissipation. If the typical length scale of the dissipating structures is l, and the typical tracer fluctuation over this length scale is $\delta\theta$, then the conditioned dissipation may be estimated as $\langle |\nabla \theta|^2 \rangle_\theta = \delta\theta^2 / l^2$. So, the salient questions are: What is $\delta\theta$? What is l? How do they depend on θ?

The second equality in (7) and (8) implies a relation between the conditional diffusion and the conditional dissipation, namely,

$$\langle \nabla^2 \theta \rangle_\theta = \partial_\theta \langle |\nabla \theta|^2 \rangle_\theta + \langle |\nabla \theta|^2 \rangle_\theta \partial_\theta \ln(P), \tag{9}$$

so that the two quantities are not independent. This relation was also derived by Nakamura,[8] in a study of atmospheric tracer mixing. Note that Eq. (9) is purely kinematic; it proceeds directly from integration by parts, and is independent of the equation that governs the evolution of θ. The relationship between conditional dissipation and conditional diffusion is dependent on the tracer PDF. If $P(\theta)$ is Gaussian and $\langle |\nabla \theta|^2 \rangle_\theta$ is independent of θ, then $\langle \nabla^2 \theta \rangle_\theta$ is proportional to $-\theta \langle |\nabla \theta|^2 \rangle_\theta$. Alternately, Eq. (9) can be solved for P, in which case it yields an expression for the PDF in terms of an integral over the ratio of conditional diffusion to conditional dissipation.[9] Being kinematic, the resulting expression is valid for any twice-differentiable field θ. It would work as well for a digitized image of the Canadian Olympic hockey team as it would for an advected-diffused tracer evolving under Eq. (1).

Equations (7) and (8) are exact, but they make the problem of representing the evolution of $P(\theta)$ look a bit simpler than it really is. The hidden problem is that the conditional averages, such as $\langle \nabla^2 \theta \rangle_\theta$, are not actually functions of θ, but are actually fluctuating quantities, whose fluctuations need to be characterized, and whose fluctuations can affect the evolution. This is especially serious on the tails of the distribution, where the fluctuations can be large compared to the mean. Previous work on the PDF transport equation does not seem to have appreciated this point. The importance of the fluctuations can be immediately grasped through consideration of the case of white noise forcing without either advection or diffusion, *viz.* $\partial_t \theta = f$, in which f has zero spatial and ensemble mean. This equation is the familiar random-walk problem, and it is a classic result that the PDF of θ is governed by a diffusion equation. Yet, the PDF transport equation obtained as a special case of (7) is

$$\partial_t P(\theta, t) = -\partial_\theta \{ P(\theta) \langle f \rangle_\theta \} \tag{10}$$

and the mean value of $\langle f \rangle_\theta$ over the ensemble of realizations is zero, leading to no evolution of P at all. The resolution of this conundrum is that $\langle f \rangle_\theta$ has nonzero values in any particular realization, and that the fluctuations entirely govern the evolution of P. To make it explicit how the fluctuations come into the picture, note that $P(Z) \langle f \rangle_\theta = \langle f \delta(Z - \theta) \rangle$, whence

$$\begin{aligned} \partial_t \langle f \delta(Z - \theta) \rangle &= -\langle f \delta'(Z - \theta) \partial_t \theta \rangle \\ &= -\partial_Z \langle f^2 \delta(Z - \theta) \rangle \\ &= -\partial_Z \{ P(Z) \langle f^2 \rangle_Z \}. \end{aligned} \tag{11}$$

Now suppose that the statistics of f are homogeneous, and that its spatial correlation is small enough that each contour of constant Z averages enough fluctuations that $\langle f^2 \rangle_Z = \langle f^2 \rangle$ is independent of Z. Suppose further that f remains constant over a time Δt, after which it switches to a new randomly

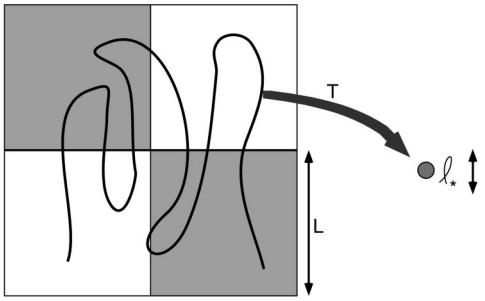

FIG. 1. Schematic illustrating the range of initial concentrations that are mixed together to make up the concentration θ near a specified point, after a time T has passed.

chosen value. Then, upon integrating (11) in time, assuming $\langle f \rangle_\theta$ to be initially zero, one finds that the *time-averaged* conditional forcing appearing in (10) is

$$\overline{P(\theta)\langle f\rangle_\theta} = -\frac{\Delta t}{2}\langle f^2\rangle \partial_\theta P, \tag{12}$$

in which the overbar denotes a time average over the interval ΔT and we have relabeled the dummy variable Z back to θ. Substitution in (10) yields the familiar diffusion equation. The point of this exercise it not to rederive the diffusion equation, but to emphasize that fluctuations in the terms $\langle \nabla^2 \theta \rangle_\theta$ and $\langle |\nabla \theta|^2 \rangle_\theta$ appearing in (7) and (8) lead to strong modifications in the evolution and equilibrium shape of $P(\theta)$.

B. Theory of the decaying case

A basic understanding of the PDF for the decaying case is obtained by examining a small well-mixed parcel at time T and looking backwards in time to see where this fluid came from, and which initial concentrations were mixed together to make the final concentration. We will assume that the size of the test parcel is the dissipation scale l_* appropriate to the point where it is located. Suppose now that the FTLE for *backwards in time* trajectories of length T emanating from the point is Λ. Then, the mixed parcel originated from a long filament of fluid of length $l_* \exp(\Lambda T)$ snaking randomly across the initial domain, as depicted in Fig. 1. This filament samples the initial range of concentrations, and the longer the filament, the more independent concentration values are mixed together to make up the final concentration. When the filament is long, the PDF of the final concentration, for given Λ, is determined by the central limit theorem. For definiteness, suppose that the initial concentration pattern is a checkerboard with square size L, and that each square is colored with alternately $\theta = 1$ or $\theta = -1$. Then, the final concentration is the mean of approximately $N = (l_*/L)\exp(\Lambda T)$ independent randomly chosen terms, each of which has the value $+1$ or -1. By the central limit theorem, the PDF of this mean is Gaussian, centered on zero, and has variance proportional to N. The argument generalizes to an arbitrary initial condition with spatial correlation length L. As time goes on, the PDF collapses exponentially to a spike centered at zero concentration. Further, for fixed time, the trajectories with large Λ have anomalously small concentration values, while the large fluctuations are due to anomalously small Λ.

To get the concentration PDF from this argument, we start with the concentration PDF conditional on Λ, which is

$$P(\theta|\Lambda) \sim \exp\left(-b\frac{l_*}{L}e^{\Lambda T}\theta^2\right) \tag{13}$$

$$\sim \exp\left(-b\frac{l_*}{L}e^{(\Lambda-\Lambda_0)T}\tilde{\theta}^2\right), \tag{14}$$

where $\tilde{\theta} = \theta \exp(\Lambda_0 T/2)$. We then convolve it with the PDF of Λ. Since the incompressible system is time reversible, then the statistics of FTLE for the reverse-trajectory problem are the same as that for the forward problem. The desired convolution is

$$P(\theta,T) = \int_0^\infty Q(\Lambda,T)P(\theta|\Lambda)\, d\Lambda \tag{15}$$

$$\sim \int_0^\infty \exp\left\{-\left(a(\Lambda-\Lambda_0)^2 T + b\frac{l_*}{L}e^{(\Lambda-\Lambda_0)T}\tilde{\theta}^2\right)\right\} d\Lambda. \tag{16}$$

In the second equality, we have assumed the Gaussian form of Q given in (4), but other forms can be used if they are available from some other theory. What we do next is rather dependent on the specific form of Q, and, more specifically, how rapidly it collapses onto a spike with increasing T.

At large T we may approximate the integral in (16) using steepest descent. The exponent is minimized when

$$2a(\Lambda-\Lambda_0) + b\frac{l_*}{L}e^{(\Lambda-\Lambda_0)T}\tilde{\theta}^2 = 0. \tag{17}$$

We have neglected some terms arising from $dl_*/d\Lambda$, which vanish at large T. For any fixed T, the statistics are then dominated by trajectories with a unique $\Lambda = \Lambda_0$ if $\tilde{\theta}^2$ is sufficiently small. However, for any fixed $\tilde{\theta}^2$, the statistics become dominated by $\Lambda \ll \Lambda_0$ at large T, and this happens exponentially quickly. Thus, the range of $\tilde{\theta}^2$ dominated by a fixed Λ_0, and for which the PDF is hence Gaussian, vanishes as T gets large. In fact, (17) implies that the PDF is eventually controlled by negative Λ, which is a spurious result, since the maximum FTLE is always non-negative. In reality, the Gaussian form of Q breaks down near $\Lambda = 0$, so that optimization argument really tells us that the behavior of the concentration PDF at long times is governed by the scaling of the PDF of Λ for small Λ. The anomalous almost-nonchaotic orbits give the remanent concentration fluctuations that are most reluctant to give up the ghost, and dominate the long-time concentration pattern. Antonsen *et al.*[10] found that the power spectrum for the decaying case was influenced strongly by those initial concentration gradients which are poorly aligned with the principal axis of the strain; similar considerations are likely to come into play for the concentration PDF as well. The general implication of (17) is that in the long term, the PDF for the decaying case should

have no Gaussian core, and should have fat tails whose specific form is determined by the behavior of $Q(\Lambda,T)$ near $\Lambda=0$.

The analysis of the decaying case in terms of the PDF transport equation plays out as follows. This case works out most readily in terms of the conditional dissipation form (8). Let $\sigma(t)$ be the standard deviation of θ, and introduce the assumption that $\mathrm{Pe}^{-1}\langle|\nabla\theta|^2\rangle_\theta = G(\theta/\sigma)\sigma^2$, where G is presumed time invariant. Then, the PDF transport equation in the absence of forcing can be cast in the form

$$\partial_\tau P + \partial_\theta\{(\partial_\theta G)P\} = -\partial_\theta\{G\partial_\theta P\}, \tag{18}$$

where $d\tau = \sigma^2 dt$. Note that if σ decays faster than t^{-1}, then the limit $t\to\infty$ corresponds to a finite value of τ, say τ_∞. Note that this is an advection-diffusion problem for P, but with *negative diffusivity*, which makes the problem exceedingly ill posed. Short waves in the initial condition amplify with a growth rate that is quadratic in the wave number, with the result that solutions become singular after a finite time unless the initial data is exceedingly smooth—specifically, having a spatial power spectrum that decays faster than a Gaussian with respect to wave number. Consider the special case $G=\text{const}$. Then, it is only the special initial condition $P\sim\exp(-\theta^2/(2\tau_\infty))$ that collapses to $\delta(\theta)$ at $\tau=\tau_\infty$, as can be seen by running a conventional diffusion equation backwards in time. This special solution corresponds to a Gaussian form of P whose width collapses to zero exponentially as $t\to\infty$. More generally, if G increases monotonically with $|\theta/\sigma|$, then the advection term on the left-hand side of (18) has the effect of expelling probability from the vicinity of $\theta=0$, leading to fat tails in the distribution.

The more typical theoretical approach to $P(\theta,t)$ for the decaying case is to seek a particular solution of the form $P(\theta,t)=P_1(\theta/\sigma)/\sigma$, which can be done consistently if σ decays exponentially with time. With this transformation, a closed form for P_1 in terms of G can be found; if G is constant, then P_1 is Gaussian, and if G increases with increasing $|\theta|$, then the PDF has tails which decay more slowly than a Gaussian.[6,7,11] The discussion of (18) shows that this particular solution is not actually the end-state of (18) for arbitrary initial data, a point that does not seem to have been appreciated previously. The time variation of G, and perhaps also its stochastic fluctuations, are crucial to mediating the approach to the asymptotic behavior.

Naive scaling would suggest that $\langle|\nabla\theta|^2\rangle_\theta$ scales like σ^2/l_*^2, where G is expected to be a constant to the extent that the value of Λ (and hence l_*) dominating the dissipation is the same for all θ. Moreover, given (5), G becomes independent of the Peclet number, since a larger Peclet number is exactly offset in the dissipation term by a smaller dissipation scale. It has been hypothesized[6,7] that $G(\theta/\sigma)$ increases quadratically with increasing $|\theta/\sigma|$, but no theoretical justification of this expectation has been advanced. The filamentary-sampling argument summarized in Fig. 1 provides some rationale for the expectation that $P(\theta)$ for the decay case will be non-Gaussian, with perhaps very little Gaussian core. From the standpoint of rigor, this argument leaves something to be desired, but it does not seem to have been made previously and it provides some useful intuition. Some more precise results on the decaying problem have been recently obtained by Balkovsky and Fouxon.[12]

C. Theory of the stochastically forced case

The starting point for the analysis of the forced problem is the observation that, in the absence of diffusion, (1) reduces to $d\theta/dt=f$, which can be solved following an individual trajectory, independently of what is happening on other trajectories. If f is suitably random following the trajectory, then the equation describes a Brownian motion process for θ. Thus, for an ensemble of trajectories that have run for length T, the PDF of θ is Gaussian, with variance proportional to $\langle f^2\rangle T$. In the absence of diffusion, the concentration is Gaussian, but its variance builds up without bound the longer the system is run. With diffusion, the variance only builds up until the time t_1, after which diffusion kills off further growth. It is reasonable to estimate t_1 by the dissipation time t_* given in (6). The dissipation time differs among the various trajectories, since t_* is a function of Λ. To the extent that the behavior is dominated by a single value of Λ, then $P(\theta)$ is Gaussian, and the variance is $\langle f^2\rangle t_*$. The variance increases like $\ln(\mathrm{Pe})$ as the Peclet number is increased, yielding infinite equilibrium variance in the absence of dissipation.

Fat tails in the PDF arise from anomalously large values of t_*, corresponding to anomalously small values of Λ. However, arbitrarily small values of Λ do not dominate the PDF, because such values have exceedingly small probability, and the probability becomes yet smaller as t_* becomes large. The dominant contribution to the PDF is determined by an optimization problem similar to that which yielded (17), but in this case Λ enters through finding the optimal t_* to make a big fluctuation, whereas in the decay case the optimum is done over trajectories over a fixed time interval T. Assuming a Gaussian form of the PDF of the FTLEs, the optimization in this case yields

$$t_* = \frac{1}{\Lambda_0}\sqrt{(\ln(L/l_*))^2 + \frac{\theta^2}{a\langle f^2\rangle}}. \tag{19}$$

Since L/l_* grows like the Peclet number, (19) implies that the concentration PDF is dominated by a single t_*, and hence is Gaussian, for a range of θ which grows like the log of the Peclet number. Within this range, t_* grows and hence the concentration variance grows logarithmically with Pe. Further, for fixed Peclet number, the width of the Gaussian core is proportional to the standard deviation of the pumping magnitude. For much larger θ, the PDF is dominated by $t_*\sim|\theta|$, or equivalently $\Lambda\sim(|\theta|\ln(\mathrm{Pe}))^{-1}$. Substitution of this into the convolution for the concentration PDF yields exponential tails. Schraiman and Siggia[13] obtained a similar result, by a somewhat different argument.

To analyze the equilibrium PDF via (7), we write $P\langle f\rangle_\theta = -D\partial_\theta P$, where D is a constant quadratic in the forcing amplitude, as per (12), where the steady form of (7) becomes

$$0 = -\mathrm{Pe}^{-1}\partial_{\theta\theta}\{P(\theta)\langle|\nabla\theta|^2\rangle_\theta\} + D\partial_{\theta\theta}P. \tag{20}$$

Upon integration over θ, P drops out and one finds the rather surprising constraint that $\mathrm{Pe}^{-1}\langle|\nabla\theta|^2\rangle_\theta = D$, i.e., that in equilibrium *the conditioned dissipation is constant*. The effect of fluctuations of the conditioned dissipation can relax this constraint. Since P drops out of the conditioned dissipation form of the transport equation, one must look to the conditioned diffusion form in order to determine the shape of P. From (7) it follows that, in equilibrium,

$$D\partial_\theta P(\theta) = \mathrm{Pe}^{-1}P(\theta)\langle\nabla^2\theta\rangle_\theta. \tag{21}$$

This equation represents the balance between the tendency of the white-noise pumping to drive P to a spreading Gaussian, and the selective damping tendency of the conditioned diffusion which tends to sharpen P.

If we make the estimate

$$\mathrm{Pe}^{-1}\langle\nabla^2\theta\rangle_\theta \sim \mathrm{Pe}^{-1}\theta/l_*^2 \sim \Lambda\theta, \tag{22}$$

then the solution to (21) is Gaussian if the dominant Λ is independent of θ. This is the Gaussian-core range discussed above. Note, however, that this argument fails to capture the logarithmic growth of tracer variance with increasing Pe. For large values of θ the optimization calculation yielded $\Lambda \sim (|\theta| \ln(\mathrm{Pe}))^{-1}$, so that the conditional diffusion for large θ becomes $\mathrm{Pe}^{-1}\langle\nabla^2\theta\rangle_\theta \sim \ln(\mathrm{Pe})^{-1}\theta/|\theta|$, which is independent of θ. The corresponding solution to (21) is now exponential, rather than Gaussian. In short, the expected form of the conditioned diffusion is linear for small to moderate values of $|\theta|$, but flattens out at large values of $|\theta|$.

The form of the PDF for the white-noise forced case was obtained more rigorously by Chertkov *et al.*,[2] without the intermediary of the PDF transport equation. The same optimization problem over Λ appears, but it is used to obtain $P(\theta)$ indirectly as a limiting form of the PDF of the correlation function $\langle\theta(\mathbf{r_1})\theta(\mathbf{r_2})\rangle$; the problem is treated through evaluation of the heirarchy of moments of the correlation function.[2] Our direct derivation in terms of the transport equation, or in terms of the optimal trajectory for making a large fluctuation, is meant to shed some light on the mechanisms leading to the Gaussian core and exponential tails, and provide some physical intuition that can be of use in guiding generalizations of the theory to more complex situations, perhaps involving chemical reactions.

III. DESCRIPTION OF THE LATTICE MIXING ALGORITHM

Direct numerical simulation of the PDE (1) can be used to explore the statistics of its solutions.[14] To solve the system with the resolution required to accurately reproduce the PDF and scaling properties requires a considerable expenditure of computer resources, owing to the amount of time that needs to be spent in time-stepping the advection. In our previous work[15] a class of model problems was proposed, which retains the essential qualitative features of (1) while offering great computational economy. The essential idea is to replace the mixing action of advection by an area-preserving map iteration:

$$x \mapsto g(x,y), y \mapsto h(x,y), \tag{23}$$

where we require $\partial(g,h)/\partial(x,y) = 1$ so as to make the map area preserving. The choice of an area-preserving map retains the essential features of incompressible flow in (1), since an incompressible flow in 2D acting over a finite time induces an area-preserving map on the plane, namely the mapping of points from their initial positions to their advected positions some time later. The map (23) induces a rearrangement of the concentration field $\theta(x,y) \mapsto \theta(g(x,y),h(x,y))$. This rearrangement alters the PDF of the gradient of θ, but does not affect $P(\theta)$ itself, since concentration is not allowed to mix between one parcel and another. This mixing is accomplished in a diffusion step, which is alternated with (23), and if there is to be a source of tracer variance, it is also inserted in this step. The mixing and forcing step may be expressed abstractly as

$$\theta \mapsto S\theta + f_n(\theta,x,y), \tag{24}$$

where S is a linear smoothing operator which damps small scales more strongly than large scales, e.g., ∇^{-2}, and f represents the action of the forcing applied at iterate n, which may simply be a random or ordered increment added to the tracer field.

The advection step (23) can be carried out with concentration tagged to a finited number of particles that are allowed to go wherever the map takes them from one iteration to the next, and the associated concentration field can be interpolated to a regular grid at the end for graphical purposes if desired. However, the smoothing operator is most easily implemented if the concentration field is available on a regular grid. For this reason, in our earlier formulation[15] the concentration field was reinterpolated to a regular grid $\{(x_i,y_j), i=1,\ldots,n_x,\ j=1,\ldots,n_y\}$ after each advection step, whereafter the diffusion step was applied in the form of a four-point smoother $\theta(x_i,y_j) \mapsto \theta(x_i,y_j) + D_{ij}$, where

$$D_{ij} = \tfrac{1}{4}(\theta(x_{i+1},y_j) + \theta(x_{i-1},y_j) + \theta(x_i,y_{j+1}) + \theta(x_i,y_{j-1})) - \theta(x_i,y_j). \tag{25}$$

This is also the dissipation employed in the present work. If there are N lattice points in each direction, and if the characteristic length scale over which the advecting fields g and h vary is that of the whole domain, then the effective Peclet number corresponding to this dissipation is N^2.

The interpolation step introduces a spurious source of tracer variance which can interfere with the long-term simulation of a freely decaying tracer field, and can obscure the effect of the true forcing imposed in (24).

High-order interpolation schemes could be used to minimize the spurious interpolation noise source, as was in effect employed in the Fourier space method of Antonsen *et al.*[10] In the present work we instead modify the map (23) slightly so as to coerce it onto a lattice, and thus eliminate the interpolation error entirely. The same trick has been employed with success in an undiffused flame propagation study.[16] We will illustrate the method for the special case of an alternating direction shear flow and a Cartesian lattice, but some generalizations will be suggested in the discussion. Consider the map

$$x \mapsto x + u_n(y), y \mapsto y + v_n(x), \tag{26}$$

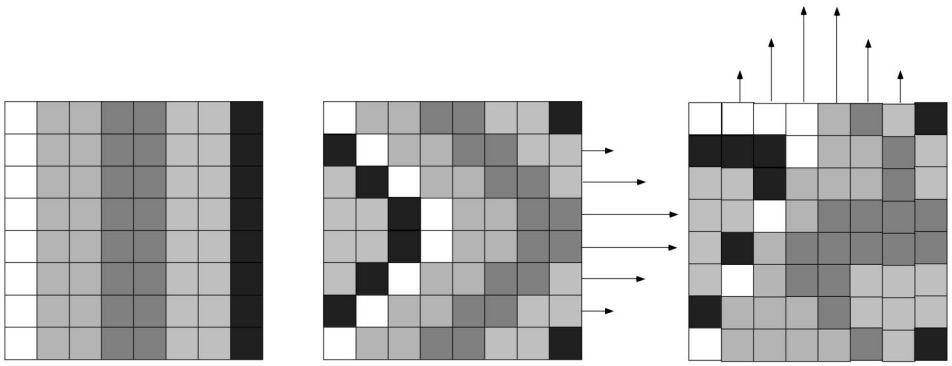

FIG. 2. Schematic of the advection step on a lattice, showing rearrangement by the composition of a shift operation in the x-direction followed by a shift operation in the y-direction.

where n is the iteration index, and the map of y is understood to make use of the updated value of x. This is manifestly area preserving; the ''standard map'' is a special case of this class of maps. Because u_n and v_n are continuous functions, if (x,y) is originally located on the discrete lattice, its image will not in general lie on the lattice. If we adopt a regular grid with spacing $(\Delta x,\Delta y)$, then by slightly modifying the map (26), we can define a nearby map that bijectively maps the lattice to itself. The required modified map is

$$x \mapsto x+[u_n(y)/\Delta x]\Delta x, y \mapsto y+[v_n(x)/\Delta y]\Delta y, \qquad (27)$$

where $[\ldots]$ is the nearest-integer function. The associated concentration is shuffled along the lattice like tiles in the familiar puzzle-tray, or like colors on the surface of a Rubik's cube. An example is shown in Fig. 2.

The lattice-rearrangement representation of the advection step has the desirable consequence that the advection step by itself *exactly* preserves $P(\theta)$. This property is difficult or impossible to achieve for numerical representations of the advection operator $\mathbf{v}\cdot\nabla$ appearing in (1). Exact preservation of $P(\theta)$ is equivalent to conserving all the moments of θ, which is a property the exact solution of (1) has in the limit $f=0$, $\mathrm{Pe}\to\infty$, but which numerical solutions have not been able to reproduce. A further advantage of (27) is that it can generally be implemented as a shift operation on the rows and columns of the matrix of values of θ, so that the advection step does not require any floating point operations at all. Simulations can therefore be carried out at very high resolution, with modest expenditures of computer time.

Some interesting aspects of the ergodicity problem are revealed starkly when thought of in terms of the lattice model. For example, one may raise the question as to whether every possible state of an $N\times N$ lattice can be reached from an initial state via a sequence of shift operations of the form in Eq. 27. If not all states are accessible, one would like to know the number of distinct equivalence classes of mutually accessible states the set of shift maps defines, and the minimum and average number of transformations needed to take one given state into another accessible one. One could inquire as to whether the set of all states accessible from a given condition are in some sense dense in the space of all lattice configurations. With regard to applications to statistical mechanics on the lattice—and perhaps to statistical mechanics in general—it must be remarked that questions of ergodicity are perhaps academic. A 1000 $\times 1000$ lattice can be rearranged in $10^6!$ or roughly $10^{6\,000\,000}$ ways. This is unimaginably greater than the number of picoseconds since the beginning of the Universe. In fact, if the entire mass of the Universe were converted into a parallel processor with each element having the mass of an electron, and if each processor processed one lattice state per picosecond since the beginning of time, only around 10^{100} lattice states would have been examined. Clearly, any attainable physical system or simulation thereof samples only an insignificant proportion of the totality of states of the system, so that the relevance of true ergodicity seems obscure. What is more at issue in statistical arguments is whether a sparse sampling of an enormous phase space provides stable estimates of the gross statistical properties in which one is interested, as if most of the vast number of states are in some sense alike.

Following our earlier work,[15] we shall study mixing in a doubly periodic domain, induced by the shear

$$u_n(y)=4\sin\,(y+\phi_n), \quad v_n(x)=\sin\,(x+\psi_n), \qquad (28)$$

where ϕ_n and ψ_n are independent random phases chosen in the interval $[0,2\pi]$. The randomization was employed so as to break up invariant tori and assure ergodicity over the whole domain. The consequences of the presence of tori and other transport-inhibiting structures are interesting, but will be left to future work. A small deviation from the original map[15] is that we now randomize the phase of both shears, rather than just one of them. This had little impact on the forced equilibrium cases, but was found to be necessary in the simulation of the very long-term behavior of the decaying case.

In the following, we present results for the freely decaying case $(f=0)$ with a large-scale initial condition, and for two flavors of forced-equilibrium cases. The first type of forced case, and the one we will emphasize, is simple additive forcing, in which f_n is a specified function of space and iteration. It could be made a random function of space and time with a definite spatial and temporal correlation length, but in pursuit of somewhat greater relevance to problems of physical relevance, we chose the steady large-scale increment $f(y)=\sin\,(y)$. Since the trajectories are chaotic, the

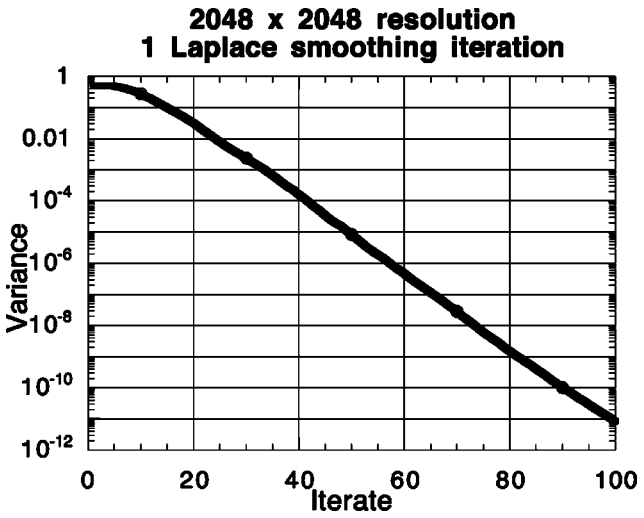

FIG. 3. Concentration variance as a function of iteration for the freely decaying cases at 2048^2 resolution.

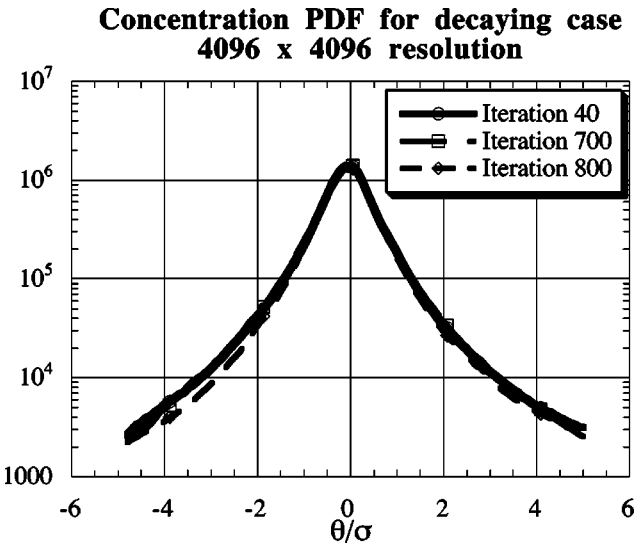

FIG. 4. Concentration PDF as a function of concentration normalized by its standard deviation, for the decaying case with 4096^2 resolution.

time series of forcing seen by a particle should be random even though f itself is fixed and ordered, so that in the Lagrangian sense the forcing is expected to be random enough that the behavior of the system is in most regards as one would expect for random forcing in the Eulerian sense. The numerical results will bear out this expectation. As noted elsewhere,[15] additive forcing is rather unlike the physical source appearing in realistic tracer problems, since realistic tracer sources tend to ''reset'' the value to certain saturation concentrations when the parcel wanders into a source region. For this reason, we also present a few results with a ''resetting'' forcing (ineptly called ''multiplicative'' formerly[15]), in which θ is reset at each iteration to $+1$ for particles residing in a strip of width ϵ centered on the lower half of the domain, whereas θ is reset to -1 for a similar strip centered in the upper half of the domain. For resetting forcing, the concentration is strictly bounded between $+1$ and -1, whereas there is no *a priori* bound for the additive case.

IV. RESULTS OF NUMERICAL SIMULATIONS

A. Concentration PDF for freely decaying case

In Fig. 3 we show the concentration variance as a function of time in the decaying case. As argued in our earlier work[15] after an initial adjustment period during which the tracer variance cascades down to the dissipation scale, the variance decays exponentially with time, at a rate that is order unity, even though the Peclet number is large. We argued further that because of the scaling of l_* with Pe, the decay rate would be independent of Pe, and would be on the order of the dominant Lyapunov exponent. Subsequent work with a reduced wave number model[10] has confirmed the generality of the decay, and has also shown that the Lyapunov exponent that determines the decay is systematically shifted by a finite amount from the most-probable exponent, despite the fact that (4) collapses onto its mode at large times. With the continuous-space map,[15] the decay is only seen for a limited time before interpolation noise halts further decay. For the lattice map results shown in Figure 3, the exponential decay continues down to machine precision. Obviating the necessity of high-order interpolation schemes, the lattice map is both efficient and easy to generalize to arbitrary shear fields.

The PDF of normalized concentration $\theta/\sigma(t)$ for a 4096^2 simulation is shown in Fig. 4 at a number of times. The PDF attains a time-independent form, and is highly non-Gaussian. There is a small Gaussian core, in the sense that the logarithmic probability is parabolic near the peak, but this range is exceedingly small; the logarithmic probability is concave except very near the peak. Numerical results quoted by Yakhot *et al.*[7] suggested that the Gaussian core grows slowly with time, but this does not seem to be the case for smooth advection-diffusion simulated at high resolution. Moreover, dominance of the non-Gaussian behavior everywhere at long times is consistent with the role of the anomalously low Lyapunov exponents discussed in connection with (17). The fat tails in the decaying case are slower than Gaussian, and in fact even slower than exponential tails. This is also to be expected from (17). No theoretical arguments have ever been put forth for exponential tails in the decaying case; Sinai and Yakhot[6] only produce a PDF whose tails look exponential over a limited range, and even that is based only on an arbitrarily specified form of the conditional dissipation. Our previous simulations of the decaying case[15] suggested exponential tails, but in retrospect this appearance was due to the limited dynamic range of θ and the relatively short times which could be treated with the continuous-space map.

The self-similar form of the PDF implies that $\langle \theta^n \rangle$ decays like $\exp(-\gamma_n t)$ with $\gamma_n \sim n$. This result is inconsistent with theoretical results on the decaying case obtained by Balkovsky and Fouxon,[12] which state that for sufficiently large n, γ_n should be independent of n. It is possible that the discrepancy arises because the behavior calculated by Balkovsky and Fouxon arises from values of θ so far out on the tail of $P(\theta)$ that they are not resolved in the numerical calculation. Balkovsky and Fouxon also note that their Eq. (3.9), which gives the form of γ_n, becomes invalid as the

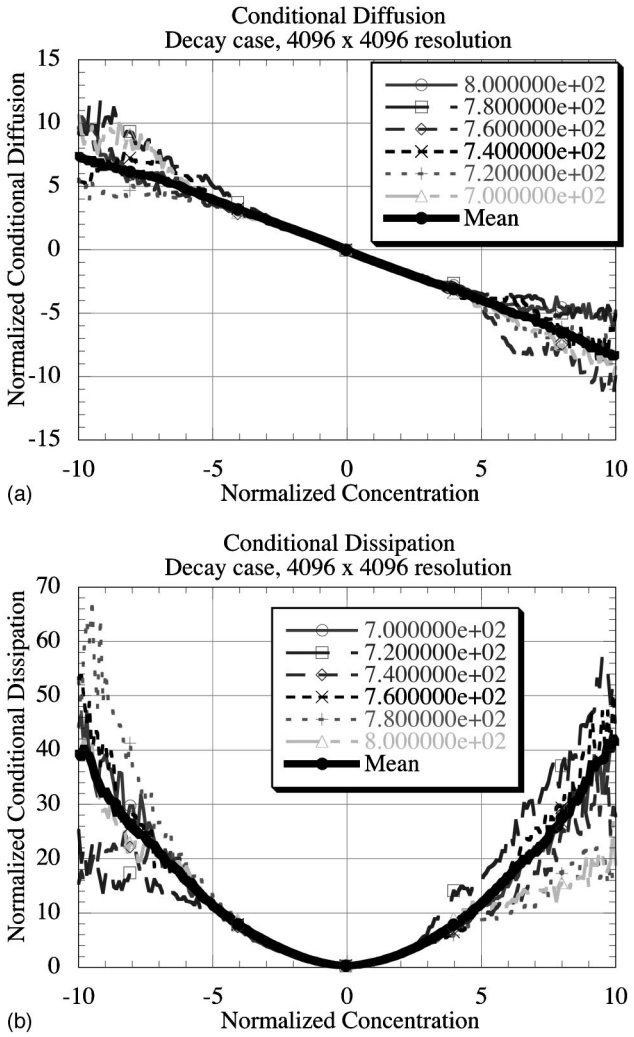

FIG. 5. Normalized conditional averages of dissipation and diffusion for the decaying case with 4096^2 resolution. Results are shown as a function of concentration normalized by its standard deviation σ. Conditional diffusion is normalized by σ, while the conditional dissipation is normalized by σ^2.

correlation time of the advecting flow increases. The lattice map we consider is equivalent to a flow with correlation times comparable to the inverse Lyapunov exponent, so that the system is not close to the δ-correlated limit. We speculate that the self-similar PDF is characteristic of advection-diffusion by flows with moderately long correlation times.

The conditional diffusion and dissipation are shown in Fig. 5 at several times. It is noteworthy that the quantities exhibit strong fluctuations for the larger values of θ/σ, which as we have argued, affects the forms of the tails of the concentration PDF. The conditional dissipation shows very strong variations with θ/σ, which is consistent with (and indeed leads to) the strongly non-Gaussian PDF. At $\theta/\sigma = 0$, the conditioned dissipation has value 0.32, and the value rises more than two orders of magnitude at $|\theta/\sigma| = 10.0$. The mean conditional dissipation is very nearly quadratic in its argument, over the whole domain for which statistics could be reliably compiled. A phenomenological picture of this can be obtained by assuming that the length scale l of the dissipating structures is fixed for all θ, but that the typical concentration fluctuation $\delta\theta$ is on the order of σ for

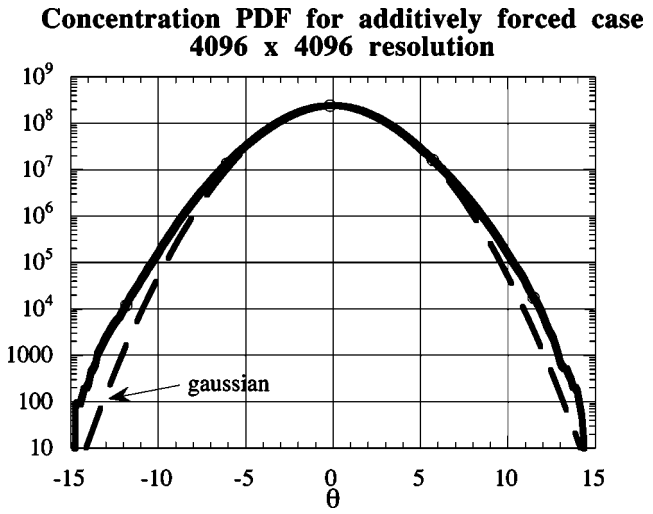

FIG. 6. Concentration PDF for the additive forcing case with 4096^2 resolution. The PDF shown is the composite of the final 700 iterations of an 800-iteration run. The best-fit Gaussian is also shown.

small θ, but becomes asymptotic to θ itself for large θ; the corresponding estimate of the normalized conditioned dissipation is then $a_1 + a_2(\theta/\sigma)^2$. The scaling of $\delta\theta$ makes sense, since for small θ the concentration of a ''neighboring'' parcel randomly chosen from the available values has a high probability of being as large as σ, but not much chance of being a lot larger. On the other hand, if we *know* a parcel has an unusually large concentration θ, then its neighbors are overwhelmingly likely to be of more normal magnitude, i.e., relatively near zero. On the other hand, the apparent constancy of l in this argument is difficult to reconcile with the optimization argument (17), which appears to require that large l dominate large fluctuations. Perhaps the growth of l is too weak to overcome the growth of the typical fluctuation. This is a matter whose definitive resolution we shall be content to leave to a future date.

The mean conditional diffusion is very linear in θ, though individual snapshots show strong fluctuations for the larger values of the argument. It must be emphasized, though, that in the *decaying* case, in contrast to the forced case, the linear part of the conditional diffusion has no bearing on the form of the concentration PDF, and in particular does not imply Gaussianity. From (7), any functional form $V(\theta)$ of the conditional diffusion simply leads to an advection equation which moves around the initial probability without causing it to converge to any unique shape. For example, if the conditional diffusion is linear in θ with a negative proportionality constant, then the equivalent velocity field just advects the initial probability towards $\theta = 0$. It is not even the deviations of the conditioned diffusion from linearity that count, but rather the effect of the *fluctuations* of the conditioned diffusion.

B. Concentration PDF for forced equilibrium case

In Fig. 6 we show the concentration PDF for the equilibrium additively forced case. It shows a very clear Gaussian core, which indeed dominates the behavior. Comparison with the best-fit Gaussian does reveal that the tails are slower

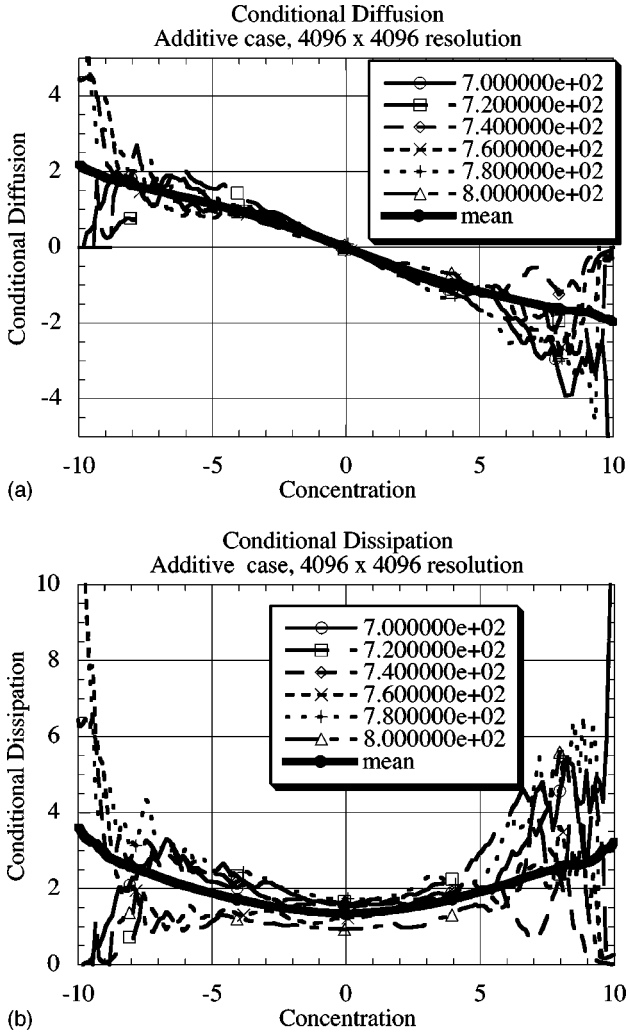

FIG. 7. Conditional averages of dissipation and diffusion for the additive forcing case with 4096^2 resolution. Results are shown for the long-term mean, and for several individual iterations.

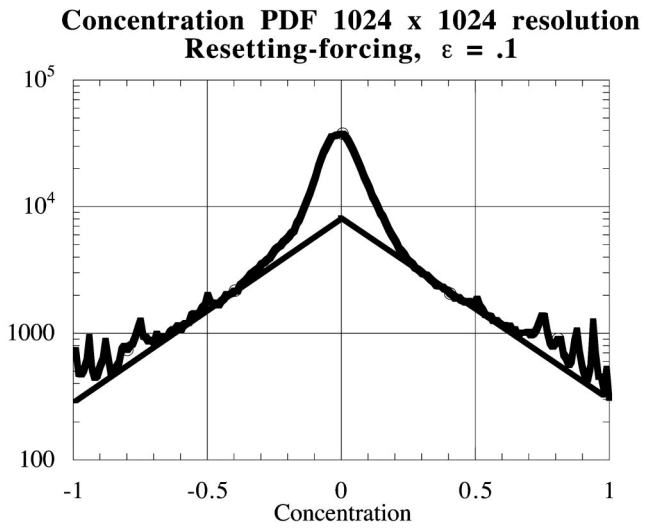

FIG. 8. Concentration PDF for the resetting-forcing case with 1024^2 resolution, at iteration 100.

than Gaussian, but we are only picking up the very beginning hints of the exponential tails required by theory. The relatively large concentrations at which the crossover to fat tails occurs is a result of the particular value of the coefficient a appearing in the Lyapunov PDF (4) for the particular advecting process employed. The coefficient enters the crossover via (19). Evidently, the value of a is large enough to nearly suppress the fat-tail behavior over the range of concentrations for which good statistics can be obtained. Processes with smaller a would show the exponential tails more prominently.

The conditional diffusion and dissipation are shown in Fig. 7. As in the decaying case, there are large fluctuations for extreme concentrations. The conditional diffusion, which is the prime statistic for the equilibrium case, is linear for small arguments, and shows the beginnings of the tendency to flatten out at large arguments. This is in accord with the fact that the fat tails only just begin to emerge in the PDF. The dissipation PDF is also shown for completeness. It is generally parabolic, but is much more constant than was the case for the freely decaying calculation. This, too, is consistent with the nearly Gaussian form of the PDF.

In earlier work,[15] we treated the equilibrium problem only for resetting forcing, and suggested that for such forcing the Gaussian core and exponential tails are not observed. We have reexamined this problem with the lattice model, with which we can better explore the long-term statistics, and have found that for suitable choice of parameters, there is a range in which behavior similar to that for the additive case can be observed. The PDF obtained with resetting strips of a width $0.1/\pi$ relative to the domain size is shown for a single time slice in Fig. 8. The behavior can be regarded as a kind of cascade in θ-space. For concentration values near those to which the concentration is reset in the strips, there are large fluctuations and nonuniversal behavior. As positive and negative values are mixed together to make smaller concentrations, the PDF begins to be governed by its asymptotic statistics. The smallest concentrations are generally the result of the largest number of mixing events, and it is here that the PDF is most Gaussian. Between this and the extreme values possible, there is an intermediate range with exponential tails.

C. Some statistics characterizing spatial structure

The shape and evolution of the function $P(\theta)$ is influenced by the spatial arrangement of the tracer, via the conditional dissipation, but it does not itself provide any direct information on the spatial structure. Some very basic information on spatial structure is encapsulated in the PDF of the dissipation field, which we shall call $P_d(|\nabla\theta|^2)$. The theory of P_d is not nearly as well worked out as that for $P(\theta)$, and it does not appear that a useful transport equation for P_d has yet been derived, even for advection-diffusion by smooth flow. For the initial value problem in the absence of forcing and diffusion, the exponential amplification of initial tracer gradients implied by (4) has the consequence that P_d should be log-normal. Diffusion substantially alters the picture, by selectively eliminating the small scale structures which typically support the largest gradients. Some theoretical results are available for smooth flow that is δ-correlated in time,[17]

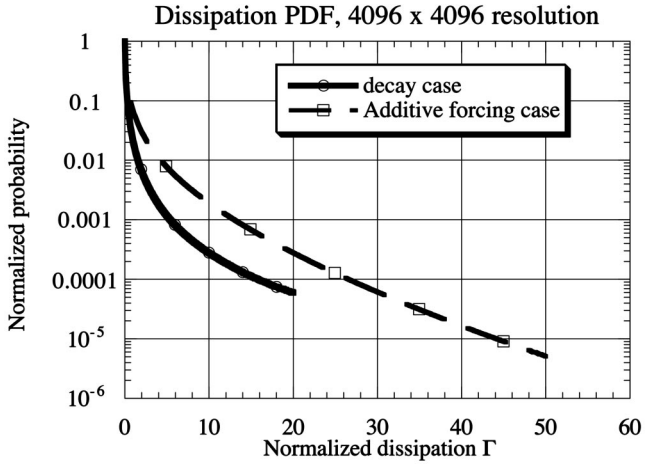

FIG. 9. Normalized PDF of the dissipation field for the decaying and additively forced cases at 4096^2 resolution. The argument is $\Gamma=|\nabla\theta|^2$ for the forced case and $\Gamma=|\nabla\theta|^2/\sigma^2$ for the decaying case, where $\sigma(t)$ is the tracer standard deviation. The gradient is based on a unit grid size. In both cases, the result shown is the long-term mean of the final 700 iterations of an 800-iteration simulation.

and these results suggest that $P_d(\Gamma)$ has a logarithmic cusp near $\Gamma=0$, and a stretched-exponential tail of the form $\exp(-c\Gamma^{1/3})$ except for extremely large Γ. The fact that the dissipation PDF is strongly affected by diffusivity makes it a good diagnostic of the influence of small scale diffusivity in experimental, observational and numerical work, in cases where the physical mechanism of dissipation is unknown or difficult to observe.

In Fig. 9 we show numerical results for $P_d(\Gamma)$, for the decaying and additively forced run discussed previously. The non-Gaussian nature of the dissipation field is immediately apparent, as a Gaussian would yield a parabola on the log-probability plot, where as the computed distribution is everywhere concave, with a cusp at small Γ. Transforming to the PDF of the gradient field itself does not eliminate the cusp or the concavity. Both the cusp and the shape of the tail are suggestive of the expectations of the theory of Chertkov *et al.*,[17] though in view of the fact that the present simulations are not for δ-correlated flow, one should not necessarily expect too close a match. Over the whole range shown in Fig. 9, the PDF can be fit almost exactly by $\exp(-c\Gamma^{0.32})$ for the decaying case and $\exp(-c\Gamma^{0.39})$ for the forced case, which are not far from the exponent predicted by theory for the δ-correlated case. On a cautionary note, it must be emphasized that the numerical results do not rule out a log-normal form of the tail. For the range of Γ shown, a log-normal fits the data nearly as well as does the stretched exponential. The essential difficulty is that Γ^{α} behaves rather logarithmically for small α, so that a very large dynamic range is needed to distinguish the stretched-exponential model from the log-normal model. This may compromise the effective use of the dissipation PDF as a diagnostic of effects of small scale dissipation.

More detailed information on spatial structure can be found from the scaling behavior of the tracer. This is characterized by the structure function

$$Z_q(\rho)=\langle|\theta(\mathbf{r}+\hat{\mathbf{n}}\rho)-\theta(\mathbf{r})|^q\rangle, \tag{29}$$

where $\hat{\mathbf{n}}$ is a unit vector in some direction. For isotropic processes it does not matter what direction we take. Knowledge of Z_q for all q is equivalent knowing the PDF of tracer fluctuations across a spatial increment ρ, provided the tails of this PDF decay at least exponentially. The second-order function Z_2 provides information equivalent to the power spectrum of θ. For scalar advection by flows with a characteristic time scale, one expects the k^{-1} Batchelor power spectrum,[18] which corresponds to $Z_2(\rho)\sim\ln(\rho/\rho_*)$, where ρ_* is an inner scale similar to the scale at which the tracer field begins to look smooth. If $Z_q=(Z_2)^{q/2}$ for all ρ, then the field is said to have ''simple scaling.'' For simple scaling, the PDF of tracer increment for any given ρ_2 can be obtained from that for another value ρ_1 by rescaling the argument of the PDF by the ratio of the standard deviations of the tracer fluctuation between the two ρ. This is a strong and convenient form of self-similarity. Any other form of scaling than this is called ''anomalous.'' It has been argued that anomalous scaling is equivalent to multifractal structure of the measure implied by the dissipation field.[15,19] The dissipation PDF, $P_d(\Gamma)$, discussed in the preceding paragraph does not have any bearing on the multifractality of the dissipation field; multifractality is a statement about how the PDF of the spatially smoothed dissipation field varies as a function of the length scale of the smoothing.

The Batchelor spectrum should apply to advection-diffusion by smooth flow, and to the advection-diffusion map for a smooth map, provided that there is enough pumping to meet Batchelor's criterion of a sufficient supply of ''θ^2-stuff.'' The decaying case does not meet this criterion, and instead has long-time behavior that settles down into a ''strange eigenmode'' that does not exhibit spatial scaling.[15] The reasons for this are now well understood, and a theory is available for the form of the strange eigenmode.[10]

It has been shown with some rigor that the Batchelor spectrum should apply to smooth advection-diffusion subject to white-noise pumping,[2] and that, moreover, the higher-order scaling should be simple rather than anomalous. The gradient measure for pure advection without diffusion can be regarded as multifractal, at least with respect to certain families of covers.[20] Our previous numerical work[15] gave indications that diffusive damping of small scales eliminated the multifractality, so that simple scaling is expected. The lack of multifractality for smooth advection-diffusion is borne out by the theory developed by Antonsen *et al.*,[10] and is in accord with the results of Chertkov *et al.*[2]

In Fig. 10 we show the structure functions for several values of q, for the equilibrium additively forced lattice model of advection-diffusion. In accordance with all theoretical expectations of this case, the second-order correlations are logarithmic, and the scaling is simple. The best fits to the behavior expected from simple Batchelor scaling are in fact plotted in the figure, but they are so accurate that the theoretical curves are hardly visible behind the simulations. In our earlier work we presented results from a model with resetting forcing, that suggested that Batchelor scaling would only be seen at exceedingly high resolution.[15] Here, we see

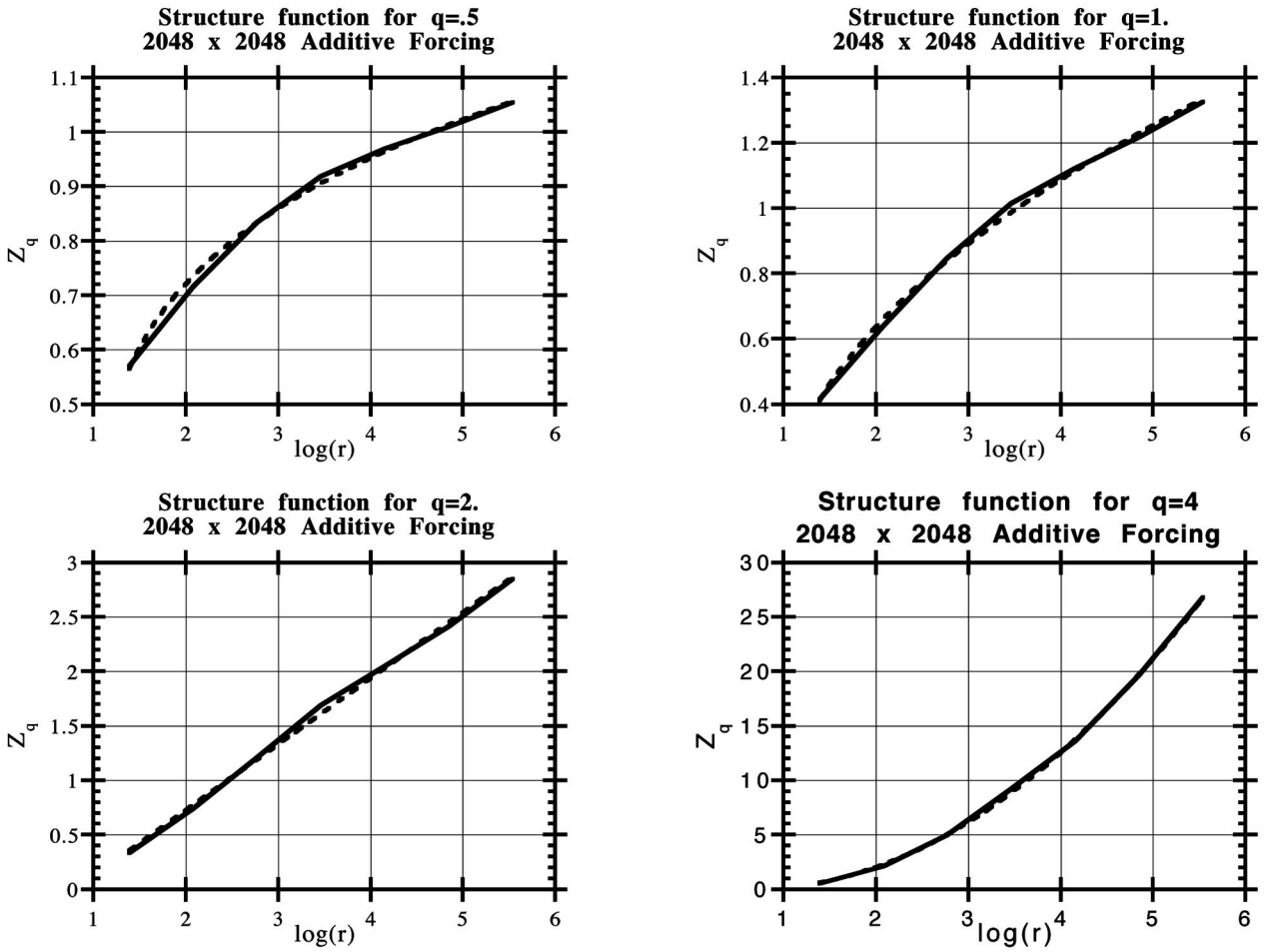

FIG. 10. Structure functions for the additively forced equilibrium case, computed with 2048^2 resolution. Best fits to the form $(\ln(r))^{q/2}$ predicted by non-anomalous Batchelor scaling are plotted, but in most cases are so exact as to be not visible on the graph.

that for additive forcing, in contrast, Batchelor scaling can be observed at resolutions that are easily achieved in two dimensions. The Batchelor spectrum is fragile, in the sense that the resolution needed to observe it is dependent on the nature of the forcing.

V. DISCUSSION

From both numerical simulations and theory for advection-diffusion for smooth flow, we have learned that the factors governing the concentration PDF differ greatly between the freely decaying case and the stochastically forced equilibrium case. For the decaying case, it is the conditional dissipation that is most important. The long-term fluctuations are dominated by trajectories with anomalously low Lyapunov exponents, there is little or no Gaussian core of the concentration PDF, and the tails of the PDF are not only non-Gaussian, but are actually fatter than exponential. The PDF of concentration rescaled by its variance attains a time-independent form.

The additively forced equilibrium case shows an extensive Gaussian core, with some indication of the theoretically expected exponential tails, even though the forcing employed is steady and spatially fixed in the laboratory reference frame. Evidently the randomization of the forcing seen by a chaotically wandering parcel is sufficient to make the system behave like the stochastically forced case. With suitable choice of parameters, the Gaussian core and exponential tails can even be seen in the ''resetting'' forcing case, where the tracer is pumped intermittently by resetting concentration to $+1$ or -1 when it enters specified regions of the domain. For any forced case, the PDF results from a balance between the action of the conditional diffusion and the conditional forcing, and the result is as much dependent on the nature of the conditional forcing as it is on the behavior of the conditional diffusion.

For either case, both numerics and theory reveal a previously overlooked consideration regarding the PDF transport equation: Fluctuations in the conditional averages of dissipation or diffusion have a strong effect on the shape of the tails of the concentration PDF. In formulating theories, these quantities need to be represented as stochastic terms fluctuating about a mean, rather than functions of concentration. The fluctuations lead to nontrivial ''eddy transports'' of probability.

The numerical simulations do not indicate that there is anything greatly wrong with the current theoretical understanding of the concentration PDF for the smooth flow case,

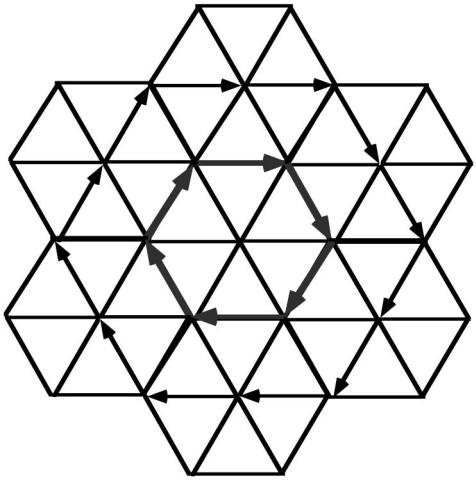

FIG. 11. Advection on a hexagonal lattice, showing the possibility of representing a vortex or rotation.

though the theory for the decaying case has some aspects that remain to be fully worked out.

Theory for the PDF of the dissipation field is not so complete. Even for smooth flow, it has only been worked out for a few special situations. Forced and freely decaying numerical experiments show a non-Gaussian form of the PDF, with stretched exponential tails and a cusp at zero dissipation. This suggests that the theory worked out for advection fields that are δ-correlated in time may be more generally valid. The numerical results for the additively forced equilibrium case also confirm theoretical expectations that the tracer field is characterized by logarithmic correlations equivalent to the k^{-1} Batchelor spectrum, and that there is no anomalous scaling.

For smooth flow, the utility of the lattice model has been demonstrated, and a few loose ends have been tied up. There have been no big surprises here. The real interest comes in the possible application of the lattice advection-diffusion model to situations where the theoretical picture is considerably more murky. The first among these to come to mind is the problem of advection-diffusion by rough flow, having singular velocity gradients. In this case, the nature of the PDF, and of the spatial scaling of the concentration field, is still a matter of considerable controversy. Some lattice model calculations for the rough flow case have been reported by Ngan and Pierrehumbert.[21] For either rough or smooth flow, the effect of nonergodicity, as manifest by various barriers to transport carving up the domain, has not been much explored. This generalization is particularly important for atmospheric and oceanic applications, in which prominent strong jets act as nearly impenetrable transport barriers.

The class of flows that can be represented in the lattice model is greatly expanded by replacing the rectangular lattice we have used with a hexagonal one, as shown in Fig. 11. With diagonal indexing, a hexagonal grid can easily be represented as a two-index array, so the only additional algorithmic baggage required is a bit more bookkeeping to keep track of all the neighbors of a given point. A hexagonal grid offers the possibility of shearing motions in three distinct directions, rather than just two, and should make the statistics more isotropic. More generally, as indicated in Fig. 11, advection by vortices centered on any grid cell can be well represented on a hexagonal grid. The possibilities are so rich that the lattice model could perhaps even evolve from a toy model to a practically useful computational scheme for incompressible advection-diffusion. The main limitation on the kinds of mixing that can be represented is that the transformation must map the lattice bijectively to itself, leaving no lattice sites unoccupied, and leaving none multiply occupied. This is no more than the expression of the incompressibility constraint, as applied to the lattice.

A further area of fruitful application of the lattice model would be in advection-diffusion problems with a chemically reacting tracer. The chemical reaction is incorporated by simply making the forcing term dependent on concentration of one or more species. From the standpoint of the PDF transport equation, one can distinguish two cases. The first case is ''weak chemistry,'' which leaves the form of the conditional diffusion unchanged from the passive case. The theory of this case is relatively easy, as nonlinear chemical reactions simply add an advection-like term to the PDF transport equation, which is easily derived from the stoichiometry of the reaction. The other case is ''strong chemistry,'' for which the chemistry significantly alters the form of the conditional diffusion. This case presents much greater theoretical challenges, and would particularly benefit from exploration using a lattice model.

ACKNOWLEDGMENTS

This work was supported by the National Science Foundation under Grant No. ATM95-05190, and also has been supported by the ASCI Flash Center at the University of Chicago under DOE Contract No. B341495.

[1] A. J. Majda and P. R. Kramer, ''Simplified models for turbulent diffusion: Theory, numerical modelling and physical phenomena,'' Phys. Rep. **314**, 238–574 (1999).
[2] M. Chertkov, G. Falkovich, I. Kolokolov, and I. Lebedev, ''Statistics of a passive scalar advected by a large-scale two-dimensional velocity field: analytic solution,'' Phys. Rev. E **51**, 5609–5627 (1995).
[3] T. Horita, H. Hiroki, I. Ishizaki, and H. Mori, ''Long-time correlations and expansion-rate spectra of chaos in hamiltonian systems,'' Prog. Theor. Phys. **83**, 1065–1070 (1990).
[4] S. B. Pope, ''The probability approach to the modeling of turbulent reacting flows,'' Combust. Flame **27**, 299–312 (1976).
[5] S. B. Pope, ''PDF methods for turbulent reactive flows,'' Prog. Energy Combust. Sci. **11**, 119–192 (1985).
[6] Y. G. Sinai and V. Yakhot, ''Limiting probability distributions of a passive scalar in a random velocity field,'' Phys. Rev. Lett. **63**, 1962–1964 (1989).
[7] V. Yakhot, S. Orszag, S. Balachandar, E. Jackson, Z-S. She, and L. Sirovich, ''Phenomenological theory of probability distributions in turbulence,'' J. Sci. Comput. **5**, 199–221 (1990).
[8] N. Nakamura, ''Two-dimensional mixing, edge formation, and permeability diagnosed in an area coordinate,'' J. Atmos. Sci. **53**, 1524–1537 (1996).
[9] E. S. C. Ching and R. H. Kraichnan, ''Exact results for conditional means of a passive scalar in certain statistically homogeneous flows,'' J. Stat. Phys. **93**, 787–795 (1998).
[10] T. M. Antonsen, Z. Fan, E. Ott, and E. Garcia-Lopez, ''The role of chaotic orbits in the determination of power spectra of passive scalars,'' Phys. Fluids **8**, 3094–3104 (1996).
[11] C. L. Valiño Dopazo and N. Fueyo, ''Statistical description of the turbu-

lent mixing of scalar fields,'' Int. J. Mod. Phys. B **11**, 2975–3014 (1997).
[12] E. Balkovsky and A. Fouxon, ''Universal long-time properties of Lagrangian statistics in the Batchelor regime and their application to the passive scalar problem,'' Phys. Rev. E **60**, 4164–4174 (1999).
[13] B. Shraiman and E. D. Siggia, ''Lagrangian path-integrals and fluctuations in random flow,'' Phys. Rev. E **49**, 2912–2927 (1994)
[14] A. L. Fairhall *et al.* ''Direct numerical simulations of the Kraichnan model: Scaling exponents and fusion rules,'' Phys. Rev. Lett. **79**, 4166–4169 (1997).
[15] R. T. Pierrehumbert, ''Tracer microstructure in the large-eddy dominated regime,'' in *Chaos Applied to Fluid Mixing*, edited by H. Aref and M. S. El Naschie (Pergamon, New York, 1994), pp. 347–366; also available as Chaos Solitons Fractals **4**, 1111–1116 (1994).
[16] J. C. Nieymeyer and A. R. Kerstein, ''Numerical investigation of scaling properties of turbulent premixed flames,'' Combust. Sci. Technol. **128**, 343–358 (1997).
[17] M. Chertkov, G. Falkovich, and I. Kolokolov, ''Intermittent dissipation of a passive scalar in turbulence,'' Phys. Rev. Lett. **80**, 2121–2124 (1998).
[18] G. K. Batchelor, ''Small-scale variation of convected quantities like temperature in turbulent fluid. Part 1, General discussion and the case of small conductivity,'' J. Fluid Mech. **5**, 113–133 (1959).
[19] S. I. Vainshtein, K. R. Sreenivasan, R. T. Pierrehumbert, V. Kashyap, and A. Juneja, ''Scaling exponents for turbulence and other random-processes and their relationships with multifractal structure,'' Phys. Rev. E **50**, 1823–1835 (1994).
[20] E. Ott and T. M. Antonsen, ''Chaotic fluid convection and the fractal nature of passive scalar gradients,'' Phys. Rev. Lett. **61**, 2839–2842 (1988).
[21] K. Ngan and R. T. Pierrehumbert, ''Spatially inhomogeneous and intermittent random advection,'' Phys. Fluids (in press).